preting i as a change in roll acceleration and/or a step change in trim angle of attack, this integration yields

$$R_x = g\sum_{i=1}^{n}\left\{\left[\frac{C_{L_\alpha}\alpha A}{W}\frac{\rho Vh}{\sin\bar{\gamma}}\right]_{av}\frac{\Gamma}{|\dot{P}|^{1/2}}\cos\left[\sigma+\theta_a-\left(\frac{\pi}{2}\right)\eta t_a'^2\right]+\frac{1}{(2\pi^{1/2})}\left[\frac{C_{L_\alpha}\alpha A}{W}\frac{\rho Vh}{\sin\bar{\gamma}}\right]_a\frac{1}{|\dot{P}|^{1/2}}\frac{\sin\theta_a}{t_a'}-\frac{1}{(2\pi^{1/2})}\left[\frac{C_{L_\alpha}\alpha A}{W}\frac{\rho Vh}{\sin\bar{\gamma}}\right]_b\frac{1}{|\dot{P}|^{1/2}}\frac{\sin\theta_b}{t_b'}\right\}_i \quad (9a)$$

$$R_y = -g\sum_{i=1}^{n}\left\{\left[\frac{C_{L_\alpha}\alpha A}{W}\frac{\rho Vh}{\sin\bar{\gamma}}\right]_{av}\frac{\Gamma}{|\dot{P}|^{1/2}}\sin\left[\sigma+\theta_a-\left(\frac{\pi}{2}\right)\eta t_a'^2\right]+\frac{1}{(2\pi^{1/2})}\left[\frac{C_{L_\alpha}\alpha A}{W}\frac{\rho Vh}{\sin\bar{\gamma}}\right]_a\frac{1}{|\dot{P}|^{1/2}}\frac{\cos\theta_a}{t'_a}-\frac{1}{(2\pi^{1/2})}\left[\frac{C_{L_\alpha}\alpha A}{W}\frac{\rho Vh}{\sin\bar{\gamma}}\right]_b\frac{1}{|\dot{P}|^{1/2}}\frac{\cos\theta_b}{t_b'}\right\}_i \quad (9b)$$

where

$$\Gamma_i = (\pi^{1/2}/2)\{[C(t_b')-C(t_a')]^2+[S(t_b')-S(t_a')]^2\}_i^{1/2} \quad (10)$$

$$\sigma_i = \tan^{-1}\{[S(t_b')-S(t_a')]/(\eta[C(t_b')-C(t_a')])\}_i \quad (11)$$

$$C(t) = \int_0^t \cos\left[\left(\frac{\pi}{2}\right)x^2\right]dx,\ S(t) = \int_0^t \sin\left[\left(\frac{\pi}{2}\right)x^2\right]dx \quad (12)$$

$$(\theta_b)_i = (\theta_a)_i + \left(\frac{\pi}{2}\right)\sum_{j=1}^{i}[\eta(t_b'^2 - t_a'^2)]_j \quad (13)$$

$$(\theta_a)_i = (\theta_b)_{i-1} \quad (14)$$

$$(t_a')_i = \left(\frac{1}{\pi^{1/2}}\right)\left(\frac{P_a}{|\dot{P}|^{1/2}}\right)_i,\ (t_b')_i = \left(\frac{1}{\pi^{1/2}}\right)\left(\frac{P_b}{|\dot{P}|^{1/2}}\right)_i \quad (15)$$

$$\eta_i = (\dot{P}/|\dot{P}|)_i \quad (16)$$

Fresnel's integrals, defined by Eqs. (12), are tabulated in Ref. 2. The functions of Eqs. (10) and (11), which contain these integrals, are presented in Ref. 1 in terms of the roll rate boundary conditions.

An interesting special case of this result is the combined effect of discontinuities in both the roll rate and trim angle of attack. That is, infinite roll acceleration or deceleration between finite roll rate boundary conditions combined with a step change in trim at the same instant. This result is described by taking the limit of Eqs. (9) as $|\dot{P}| \to \infty$ and substituting into Eq. (3) to obtain

$$R = -\left(\frac{g}{2}\right)\left[\frac{C_{L_\alpha}A}{W}\left(\frac{\rho Vh}{\sin\bar{\gamma}}\right)\right]_a\left|\frac{\alpha_b P_a - \alpha_a P_b}{P_a P_b}\right| \quad (17)$$

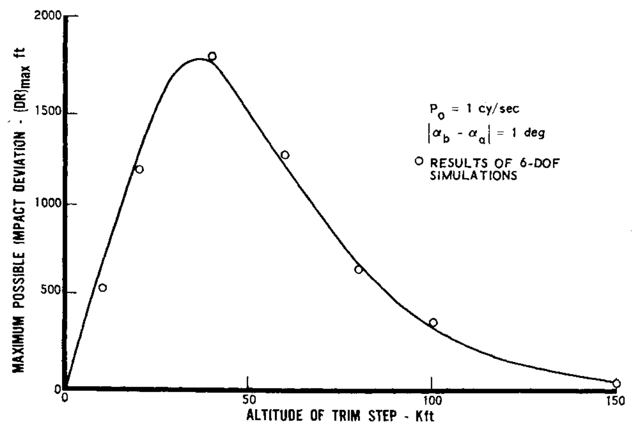

Fig. 2 Effect of a step change in lift on re-entry vehicle impact for constant roll rate.

Table 1 Combined Effect of a lift step and a roll rate variation from 1 cy/sec

Case	P_b, cy/sec	α_a, deg	α_b, deg	$[(DR)_{\max}]_{\text{Eq. 17}}$, ft	$[(DR)_{\max}]_{\text{6-DOF}}$ ft
1	$\frac{3}{2}$	0	1	1184	1126
2	2	0	1	888	856
3	3	0	1	592	605
4	$\frac{1}{2}$	0	1	3551	3304
5	$\frac{1}{2}$	$\frac{1}{2}$	1	2663	2493

Eq. (17) includes the result for constant roll rate as a special case since for $P_a = P_b$ this expression reduces to Eq. 8.

Results and Conclusions

An example of the effect of roll rate variation on the impact of a re-entry vehicle was presented in Ref. 1. That same vehicle will be used here to obtain an example of the effect of a trim step at constant roll rate on impact. The relevant physical characteristics of the vehicle are: $\beta = 2000$ psf, $W = 131$ lbs, $A = 0.92$ ft^2, and $C_{L_\alpha} = 0.034$ deg^{-1}. The re-entry velocity and flight-path angle are 22,690 fps and $-20°$, respectively. The effect of a one degree step change in trim angle of attack on impact at a constant roll rate of one cycle per second is shown in Fig. 2 as a function of the altitude at which the step occurs. These results were obtained using Eqs. (8) and (4). Included also are the results of six-degree-of-freedom trajectory simulations for comparison.

The results of Ref. 1 indicated that the effect of roll rate variation from one cycle per sec on impact for the vehicle and re-entry conditions described previously and for $|\dot{P}| \approx 50$ cy/sec^2 at an altitude of 35,000 ft were essentially the same as those for $|\dot{P}| \to \infty$ at the same altitude. Therefore, $|\dot{P}| \approx 50$ cy/sec^2 was used in various six-deg-of-freedom trajectory simulations of the combined effect of lift and roll rate variation, and compared to results using Eqs. (17) and (4) in Table 1. All of the results of this analysis compare well with the results from the trajectory simulations.

References

[1] Crenshaw, J. P., "Effect of Lift with Roll Rate Variation on Re-Entry Vehicle Impact," *Journal of Spacecraft and Rockets*, Vol. 8, No. 5, May 1971, pp. 483–488.

[2] Jahnke, E. and Emde, F., *Tables of Functions*, Dover, New York, 1945, pp. 34–37.

Ion Propulsion System: Regulation of the Vaporizer Temperature

C. LANDRAULT* AND M. BRIOT†

Laboratoire d'Automatique et de ses Applications Spatiales du C.N.R.S., Toulouse, France

Nomenclature

a = average radius of the ionizer pores
A = molecular mass of cesium
A_i = emitting area of the ionizer

Received August 3, 1971; revision received November 29, 1971.
Index category: Electric and Advanced Space Propulsion.

* Research Engineer, Ion Propulsion and Digital Technics Team.
† Dr. in Electronics, Ion Propulsion and Digital Technics Team.

e = ion charge
I_b = beam current
k = Boltzmann constant
l = average length of the ionizer pores
m = ion mass
N = Avogadro's number
T_i = ionizer temperature
T_v = vaporizer temperature
δ_p = density of ionizer pores per unit area
η_i = ionization efficiency

THE progress made in geostationary telecommunications satellites equipped with large solar panels has led the Direction des Programmes et du Plan of the Centre National d'Etudes Spatiales[1] to interest itself in the study and realization of a cesium contact ion thruster the thrust of which will be in the order of several millinewtons. One study made during this program[2,3] at the "Laboratoire d'Automatique et de ses Applications Spatiales" of the "Centre National de la Recherche Scientifique" concerns attitude control by electrostatic deflection of the ion beam.

In the design of a control law, it is necessary to know accurately the static and dynamic parameters of the thruster so as to make it operate near its normal working point during the entire mission. This necessitates a thorough understanding of the mathematical model of the thruster system, considered as a multivariable one, which permits us to see the influence of the input values on the output value, in this case, the thrust vector. The aims of this report are the following: 1) to indicate, in a theoretical form, the effect of the vaporizer temperature; 2) to prove the necessity of a control loop; and 3) to provide a detailed circuit diagram of the realized control loop.

Theoretical Study of the Effect of the Vaporizer Temperature on the Thrust Vector[4,5]

In the case of a thruster with thrust F and positive high voltage U, the beam current is given by:

$$I_b = (FN/A)\,(em/2U)^{1/2}$$

In order that the thruster should have a long life-time which requires a minimization of the neutral flux, it is necessary that the beam current should be equal to its saturation value. The latter is determined by application of the gas statistical kinematics laws:

$$I_{bs} = \alpha e \eta_i A_i p/(2kT_i \pi m)^{1/2}$$

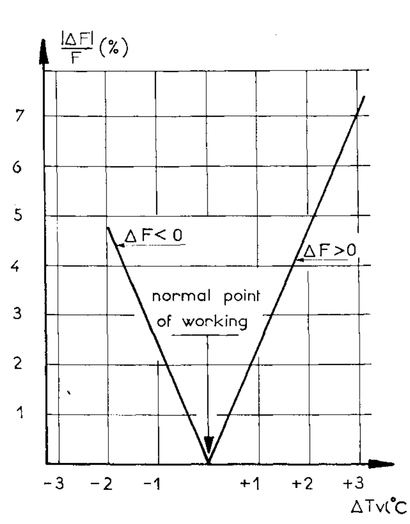

Fig. 1 Influence of the vaporizer temperature on the thrust level.

where the coefficient α is given to a first approximation by the equation derived from the Knundsen theory of rarified gases,

$$\alpha = \pi^2 a^3 \delta_p / l$$

the pressure, p, before the ionizer is a function of the temperature of the coldest point in the system, in fact the liquid-vapor interface in the vaporizer.

This pressure is given by the empirical law[6]:

$$\log_{10} p_{mm\,Hg} = 6.62 - 3{,}701/T_v$$

By equalizing I_b to I_{bs} we obtain the relation between the thrust and the vaporizer temperature:

$$F = 5.65 \times 10^8 \alpha \eta_i A_i (eU/k\pi T_i)^{1/2} \quad e^{-8{,}522/T_v}$$

As we indicated in the introduction, it is necessary to know the normal working point before studying the effect of the vaporizer temperature particularly the normal values of T_i, T_v and U. We have developed a mathematical model of the thruster in order to obtain a numerical program for optimization of the microthruster. The chosen criterion was the minimization of the total mass of the thruster and its associated electronics. For the case studied,[4] this program gave us the following values:

$$T_i = 1{,}373°\text{K}, \qquad T_v = 628°\text{K}, \qquad U = 1{,}960 \text{ v}$$

Substitution of these values in the preceding equation gives:

$$F = 1{,}700\, e^{-8{,}522/T_v}$$

The graph of $|\Delta F|/F$ against ΔT_v is given in Fig. 1. The necessity of regulating the vaporizer temperature is clearly shown. In fact, a variation of 1°C causes a variation of 2.5% in $|\Delta F|/F$. In order to maintain the relative error in the thrust at less than 1% we must regulate the vaporizer temperature to an accuracy of about 0.25°C.

Design of the Vaporizer Temperature Control Loop

Utilization of a thermocouple as a vaporizer temperature sensor is difficult in practice because of the necessity of a reference temperature for its cold solder. The same is true for the utilization of a platinum resistance thermometer due to mounting difficulties and the existence of temperature gradients in the vaporizer. Hence, we prefer to regulate the

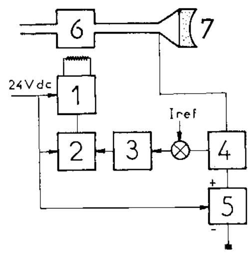

Fig. 2 Block diagram of the vaporizer temperature control loop: 1) d.c.–a.c. converter; 2) variable switching voltage regulator; 3) power limiting and control signal generation; 4) current sensor; 5) high positive voltage converter; 6) vaporizer; 7) ionizer.

beam current. The block diagram of the regulation is given in Fig. 2.

The beam current coming from block 4 which is composed of an optoelectric sensor and current-voltage amplifier is compared with the reference beam current. The error ΔI_b passes through block 3, which is composed of a power limiting system, to avoid the application of too high a power to the cold heating system, and a system furnishing the control signal. The latter drives a switching voltage regulator (block 2) which allows us to modulate the input voltage of the d.c.–a.c. converter represented by block 1.

Realization of the Vaporizer Temperature Control Loop

The circuit of the block 4 is shown in Fig. 3. On this diagram β is the d.c. current transfer ratio of the opto isolator, $V-$ and $V+$ are the supply voltages. The reference value of the beam current is fixed by the V_1 voltage and the error ΔI_b is represented by the V_3 voltage.

The switching voltage regulator of block 3 works at a frequency in the order of 10 kHz. Its efficiency is 86% for an output power of about 10 w. The ripple voltage and

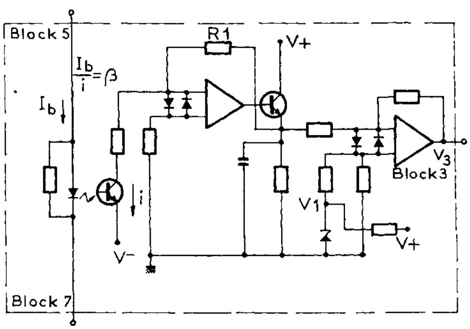

Fig. 3 Circuit diagram of the block 4.

variations in the output voltage for maximum and minimum supply voltage and load are all less than 1% of the output voltage. The graph of Fig. 4 shows the control voltage of the switching voltage regulator against the beam current. On this graph V_2 denotes the voltage controlling the threshold beam current value for which the regulation loop is closed; V_4 is the normal control voltage of the regulator.

The d.c.–a.c. converter of block 1 is composed of an oscillator driving a power stage. Its efficiency is 93% and its operating frequency is of the order 12.5 kHz for an output power of about 10 w.

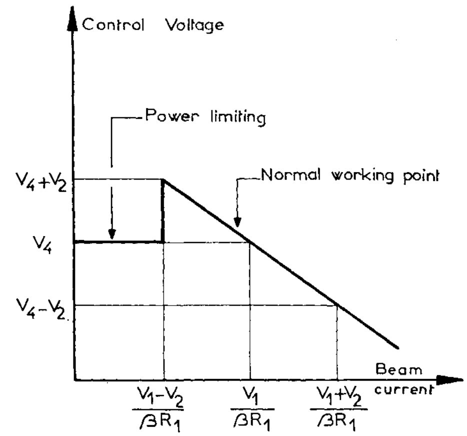

Fig. 4 Control voltage vs beam current.

References

[1] Luquet, P. and Costes, A., "Orbit Corrections and Attitude Control Systems for the Telecommunications Satellites: Development of Ion Propulsion in France," *4th Automatic Control in Space Symposium, International Federation of Automatic Control*, Survey Paper, Session 10, Dubrovnik, 1971.

[2] Lagasse, J., Costes, A. and Laprie, J. C., "Synthesis of the Studies Carried out by the Laboratoire d'Automatique et de ses Applications Spatiales du C.N.R.S. on the Satellite Stabilization by Ion Thrusters," *D.G.L.R, Symposium on Electric Space Propulsion Systems* Deutsche Gesellschaft für Luft—und Raumfahrt e. V., Paper 71–034, Braunschweig, 1971.

[3] Briot, M., Costes, A., Laprie, J. C. and Marpinard, J. C., "Convertisseur continu-continu a tension de sortie commandable destiné à des systèmes de stabilisation par propulsion ionique," 3rd International Conference on Space Technology, Paper 24, Centro Studi Trasporti Missilistici, 1971.

[4] Brewer, G. R., *Ion Propulsion*, Gordon and Breach, New York, 1970.

[5] Landrault, C., Briot, M. and Luquet, P., "Alimentations électriques nécessaires à la propulsion ionique," Note interne n° 756 du Laboratoire d'Automatique et de ses Applications Spatiales, Toulouse, France, 1971.

[6] Techniques de l'Ingénieur." Constantes physico chimiques, section K-640, Paris, 1955.